AAV-mediated MUC5AC siRNA delivery to prevent mucociliary dysfunction in asthma

Authors

<u>Sahana Kumar</u>[1], Maria Corkran[1], Yahya Cheema[2], Margaret A. Scull[1,2*], Gregg A. Duncan[1,2*]

Affiliations

[1]Department of Cell Biology & Molecular Genetics, Maryland Pathogen Research Institute (MPRI) University of Maryland, College Park, MD 20742. [2]Fischell Department of Bioengineering, University of Maryland, College Park, MD 20742.

Corresponding authors e-mail: gaduncan@umd.edu

Abstract

The main structural components of mucus produced in the lung are mucin 5B (MUC5B) and mucin 5AC (MUC5AC) where a relatively higher expression of MUC5B is typical in health. In the lungs of individuals with asthma, there is a shift from MUC5B to MUC5AC as the predominantly secreted mucin which has been shown to impair mucociliary clearance (MCC) and increase mucus plug formation in the airways. Given its role in asthmatic lung disease, MUC5AC represents a potential therapeutic target where a gene delivery approach could be leveraged to modulate its expression. For these purposes, we explored adeno-associated virus serotype 6 (AAV6), as a lung-tropic viral gene vector to target airway epithelial cells and reduce MUC5AC expression via siRNA delivery. We confirmed that AAV6 was able to transduce epithelial cells in the airways of healthy mice with high transgene expression in mucus-secreting goblet cells. Using multiple particle tracking analysis, we observed that AAV6 was capable of penetrating both normal and MUC5AC-enriched mucus barriers. Successful transduction with AAV6 was also achieved in IL-

24   13 stimulated human airway epithelial (HAE) cells differentiated at air-liquid interface (ALI).

25   AAV6 expressing MUC5AC-targeting siRNA was evaluated as a prophylactic treatment in HAE

26   cell cultures before IL-13 challenge. IL-13 stimulated HAE cultures treated with AAV6-MUC5AC

27   siRNA had significantly reduced MUC5AC mRNA and protein expression compared to untreated

28   controls. Mucociliary transport in IL-13 stimulated HAE cultures was also maintained and

29   comparable to healthy controls following AAV6-MUC5AC siRNA treatment. Together, these

30   findings support that AAV6 may be used as an inhaled gene therapy to suppress MUC5AC

31   overexpression and restore normal airway clearance function in asthma.

32

Introduction

34   Asthma is a chronic lung disease, affecting millions worldwide, adults and children alike[1].

35   Individuals with asthma typically experience coughing, difficulty breathing and wheezing which

36   impacts their day to day activities and overall quality of life[2,3]. Allergic asthma is associated with

37   airway inflammation, airway remodeling, and impaired clearance of mucus from the airway by

38   coordinated beating of cilia on the epithelium, a process known as mucociliary clearance (MCC)[4,5].

39   As asthma worsens, excess mucus is produced leading to mucus plug formations due to impaired

40   MCC[6]. Standard treatments for asthma, including corticosteroids and bronchoconstrictors, are

41   focused primarily on managing the symptoms of inflammation and airway constriction. However,

42   patients endure the disease for years and long-term use of these drugs can cause significant

43   financial burden and have off-target effects[7–9]. Beyond over-the-counter expectorants which may

44   provide temporary symptom relief, there has been minimal progress in therapeutic development to

45   address muco-obstruction and airway plugging observed in severe asthma.

46   To achieve long-lasting therapeutic effects, gene therapy strategies have been developed and

47   evaluated for their ability to inhibit or reduce specific Th2 inflammatory pathways in asthmatic

48   airways. In addition, local delivery of gene therapies for asthma via inhaled or intranasal

49   administration can enable less frequent dosing and reduce off-target effects[10]. So far, targeted gene

50   therapeutic approaches for asthma have used both viral and non-viral vectors, loaded with either

51   antisense oligonucleotides, siRNA, or mRNA that aim to antagonize or silence inflammatory

52   mediators or shift the immune response from a Th2 response to a Th1 response[11–16]. In previous

53   work, an adeno associated virus (AAV) encoding for receptor antagonist of IL-4RA was able to

54   alleviate the Th2 allergic response in a mouse model of allergic asthma. This strategy also reduced

55   mucus hypersecretion and airway hyperresponsiveness in ovalbumin sensitized mice[11]. Another

56   study used AAV for sustained expression of IL-12 to enhance Th1 responses in OVA sensitized

57   asthmatic mice where they observed reduced Th2 cytokines in treated mice[17].

58

59   While inflammation and immune mediators are an important therapeutic target, fatal asthma

60   attacks are often caused by mucus plugs which can partially or fully occlude small and large

61   airways leading to restricted airflow[18–20]. Within the lung, mucus is formed by gel-forming mucin

62   glycoproteins, mucin 5B (MUC5B) and mucin 5AC (MUC5AC) where each of these mucins

63   possess distinct biochemical (e.g., glycosylation pattern) and biophysical properties (e.g.,

64   macromolecular assembly, crosslinking)[6]. Healthy airway mucus is comprised predominantly of

65   MUC5B and with relatively lower levels of MUC5AC, while the contrary is observed in asthmatic

66   airways, with MUC5AC being the predominant mucin[21]. Prior studies have shown that this change

67   in mucus composition contributes to viscous mucus, impaired MCC, and mucus plug formations

68   in airways[18,22,23]. These prior studies also established IL-13 mediated goblet cell hyperplasia in

69   asthma leads to MUC5AC hypersecretion and pathological mucus production in asthma. A study

70   by Siddiqui et al. targeted microRNA miR-141, which regulates IL-13-induced mucus secretion,

71   and showed miR-141 disruption reduced goblet cell hyperplasia, MUC5AC expression, and total

72   secreted mucus[24]. As such, MUC5AC warrants attention as a therapeutic target for treating asthma

73   which could be addressed using a gene therapy strategy.

74

75   AAV is one of the leading viral vectors for gene therapy applications because it has broad tissue

76   tropism and is non-pathogenic. Further, several AAV-based approaches have obtained FDA

77   approval with many others in clinical trials[25,26]. To deliver MUC5AC-siRNA, AAV serotype 6

78   (AAV6) was selected for these studies based on its tropism for the lungs and ability to transduce

79   airway epithelial cells *in vitro* and *in vivo*[27,28]. We have also shown in prior work that AAV6 can

80   penetrate hyper-concentrated mucus produced by individuals with cystic fibrosis lung disease and

81   transduce airway epithelium in the βENaC transgenic mouse model of muco-obstructive lung

82   disease[29]. Building on this prior work, we determined in the current work that AAV6 can transduce

83   secretory cells in mouse airways and as such, is a relevant gene vector for MUC5AC siRNA

84   delivery. To determine its effectiveness in the context of disease, we further evaluated if AAV6

85   could successfully penetrate pathological asthma mucus for delivery of MUC5AC siRNA and

86   improve MCC in IL-13 stimulated human airway epithelial cultures. The results of this work could

87   open new avenues for inhaled therapeutics for asthma and other muco-obstructive lung diseases.

88

89   **Results**

90   *AAV6 transduction in mouse airway and lung epithelium*

AAV6 has shown tropism for airway and lung tissue with enhanced gene transfer efficiency *in vitro* and *in vivo* compared to other serotypes[28–31]. To examine and validate that AAV6 can deliver genes to target airway epithelial subtypes, we conducted an *in vivo* biodistribution study (**Fig 1**). Briefly, AAV6 encoding for an mCherry reporter was intranasally administered into 6-week-old BALB/c mice (5 males and 5 females) at a dose of 10^{11} viral particles/mouse in 15 µl PBS (**Fig 1A**) and equal volume of PBS in controls. As expected, mice in both the control and treated groups did not show any signs of adverse effects with normal weight gain observed over the course of the study (**Fig 1B**). After 14 days, mice were euthanized in order to collect trachea and lung tissue to measure mCherry expression in epithelial subtypes by flow cytometry and immunofluorescence. Immunofluorescence analysis showed mCherry expression in tracheal sections indicating successful AAV6 transduction (**Fig 1C**). Quantification of mCherry in tracheal epithelial subsets via flow cytometry indicated a significantly higher transduction in MUC5AC+ goblet cells subsets compared to basal and ciliated cells as well as increased transduction in TSPAN8+ secretory cells (**Fig 1D**). Immunofluorescence in lung samples yielded less conclusive results with low mCherry expression in immunofluorescence images of lung sections (**Fig S1A**). However, there was significantly higher transduction in TSPAN8+ epithelial cell subtypes compared to other epithelial subtypes (**Fig S1B**).
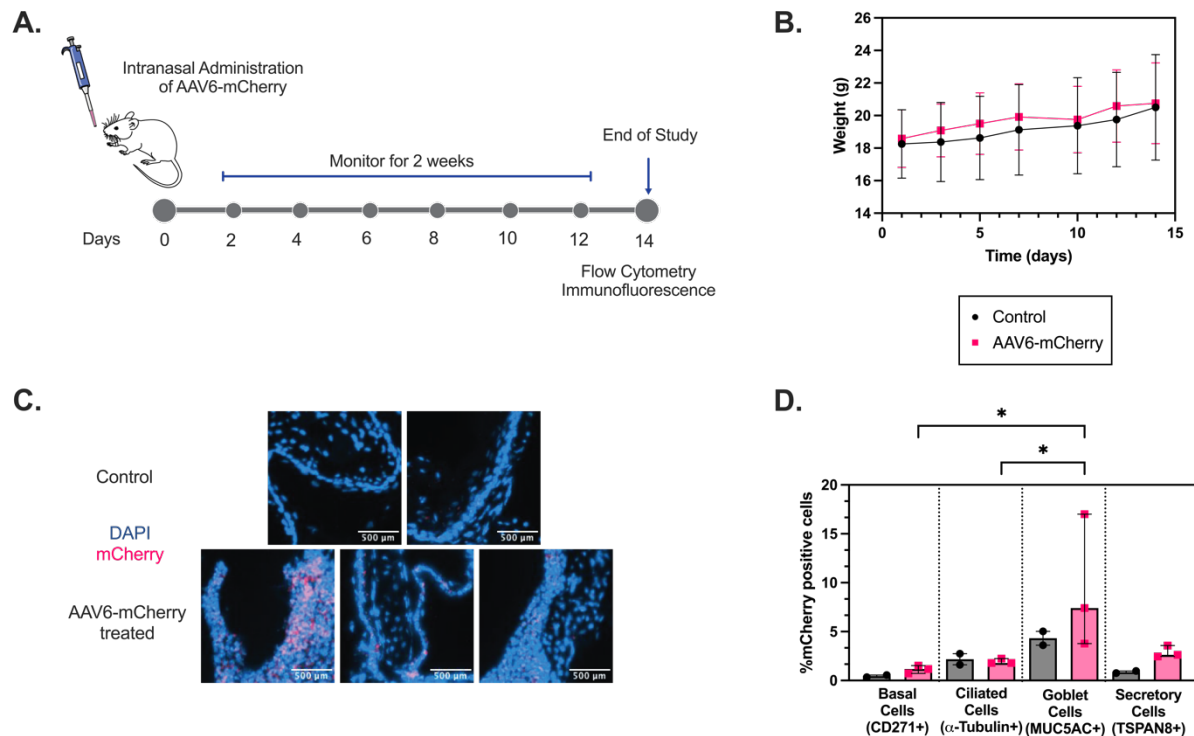
Figure 1: *In vivo* AAV6 transduction in mouse airway epithelial cells. (A) Schematic illustration showing intranasal AAV6 administration in BALB/c mice and overall study design. (B) Graph showing mouse weights which were recorded every other day throughout the study and showed a steady increase in both control and treated groups. **(C)** Immunofluorescence images of trachea sections in control (PBS) and AAV6-mCherry infected mice. mCherry transduction is shown in pink. Scale bar = 500 μm. **(D)** Bar Graphs show % mCherry positive cells normalized to control in different airway epithelial cells from single cell suspension of excised trachea. *$p < 0.05$ by Ordinary one-way ANOVA. Each dot represents results from lung tissue from one mouse.

AAV6 is diffusive in asthma-like, MUC5AC-enriched mucus

After confirming the relevance of AAV6 as a gene vector for pulmonary delivery to target mucus secreting cell types, we then characterized AAV6 diffusion in normal and MUC5AC-rich mucus produced *in vitro* from air liquid interface (ALI) cultures of human airway epithelial (HAE) cells to mimic mucus from asthmatic patients. Previous studies have shown that stimulation of HAE cultures with IL-13, which is a key cytokine in allergic asthma, causes goblet cell hyperplasia, increased MUC5AC production and reduced mucociliary transport[23,32–34]. As such, we established this *in vitro* asthma model by stimulating BCi-NS1.1 HAE cultures grown at ALI with IL-13 (10

127   ng/ml) for 7 days as previously described[22,33] (**Fig 2A**). These cultures will be referred to as IL-13

128   treated HAE cultures. We also utilized a previously established model in BCi-NS1.1 cells where

129   MUC5B gene expression is knocked-out via CRISPR-Cas9 leading to the production of

130   MUC5AC-enriched airway mucus (**Fig 2A**).[35] The diffusion of fluorescently labeled AAV6 (~20

131   nm in diameter)[36] and 20 nm diameter muco-inert nanoparticles (NP) was measured in control

132   mucus. We confirmed that the muco-inert NPs were in the same size range as AAV6 by dynamic

133   light scattering measurements. The diffusion rates for AAV6 and NPs were measured in the same

134   regions of interest using fluorescence video microscopy. Based on the multiple particle tracking

135   analysis and measured mean squared displacement at time scale of 1 second (MSD_{1s}), the diffusion

136   rate for muco-inert NPs were significantly higher than the rate for AAV6 (**Fig 2B**). We compared

137   AAV6 diffusion in regular (healthy) mucus, IL-13 mucus, and mucus from MUC5B knockout

138   (MUC5B KO) cultures, which are predominantly composed of MUC5AC to see how this change

139   in mucus composition would impact viral diffusion. We found AAV6 is diffusive and traverses

140   through the gel network comparably in control mucus, IL-13 mucus, and MUC5B-KO mucus as

141   shown by the trajectories (**Fig 2C**) and median $\log_{10}(MSD_{1s})$ values (**Fig 2D**) with no significant

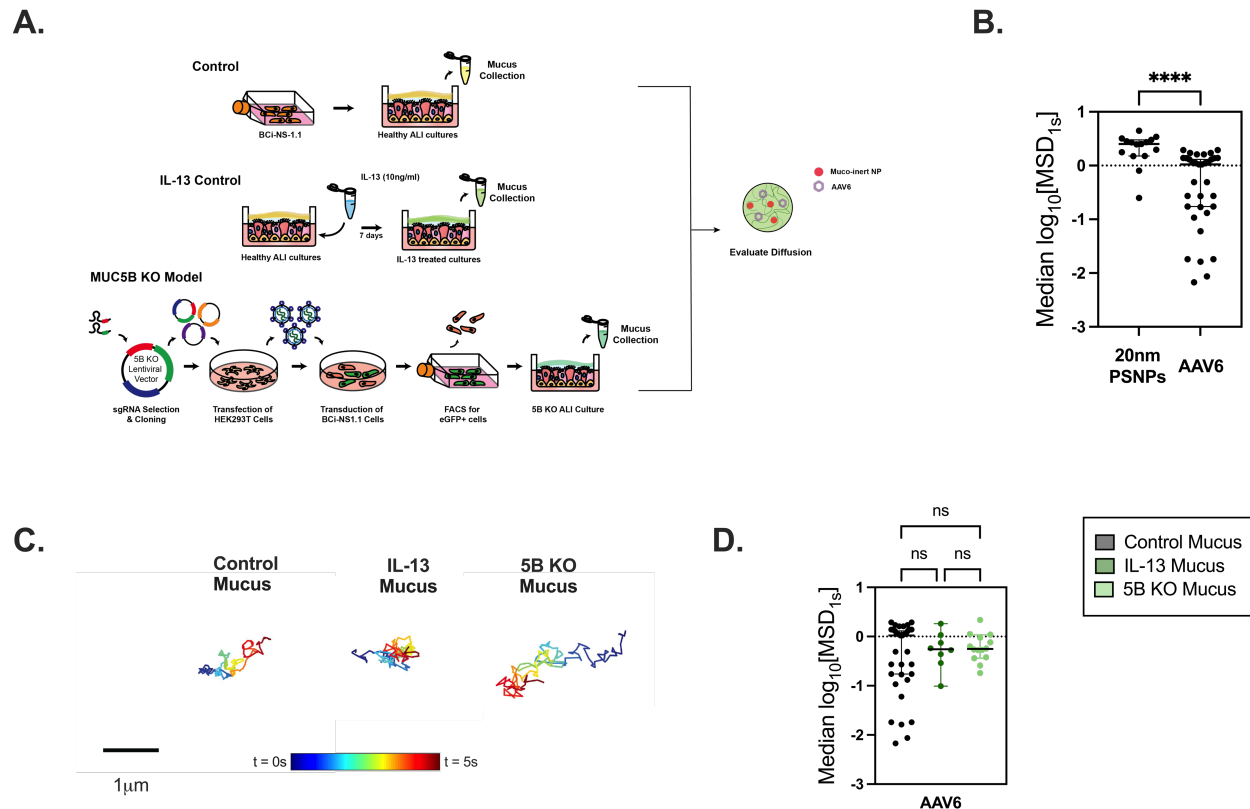142   difference between mucus types.

Figure 2: AAV6 diffusion in control and IL-13 treated mucus from *in vitro* cultures. (A) Schematic illustration showing the different *in vitro* models from which mucus was collected. BCi-NS1.1 cells were grown at ALI to establish Healthy ALI cultures. Healthy differentiated ALI cultures were stimulated with IL-13 (10 ng/ml) for 7 days to produce MUC5AC rich mucus. MUC5B KO cultures were generated using lentiviral mediated delivery of sgRNA and CRISPR-Cas9. Mucus from healthy controls, IL-13 treated cultures and MUC5B KO cultures were collected and AAV6 diffusion was measured in comparison to muco-inert nanoparticles of similar size. **(B)** Scatter plots of measured median $\log_{10}[MSD_{1s}]$ for AAV6 and 20 nm muco-inert nanoparticles in healthy mucus collected from ALI cultures. ****$p < 0.0001$ by Mann-Whitney Test. **(C)** Representative trajectories of AAV6 diffusion in control mucus, IL-13 treated mucus, and MUC5B KO mucus. Trajectory color changes with time with dark blue indicating 0 s and dark red indicating 5 s. Scale bar = 1 µm. **(D)** Scatter plots of measured median $\log_{10}[MSD_{1s}]$ for AAV6 in healthy control mucus, IL-13 treated mucus, and MUC5B KO mucus. $p > 0.05$ by Kruskal-Wallis test with Dunn's correction. Each dot represents data from 1 video (n≥3).

AAV6 effectively transduces IL-13 stimulated airway epithelial cells in vitro

We next wanted to verify that AAV6 can transduce IL-13 stimulated HAE cultures *in vitro*. We first investigated the transduction efficiency of AAV6 expressing enhanced green fluorescence protein (eGFP) in undifferentiated BCi-NS1.1 HAE cells at multiplicities of infection (MOI) of 10^3, 10^4 and 10^5. AAV6 mediated GFP expression was evaluated 72 hours post infection using

164 fluorescence imaging. Successful transduction was observed in cultures inoculated at a MOI as

165 low as 10^3, with a substantial increase in fluorescence detection with MOI of 10^4 and 10^5 (**Fig 3A**).

166 Based on this, AAV6-eGFP transduction was evaluated at MOI of 10^5 in IL-13 treated

167 differentiated ALI cultures and compared to untransduced untreated and IL-13 treated HAE

168 controls. There was evident GFP expression in transduced groups (**Fig 3B**). The GFP integrated

169 density was evaluated in AAV6-eGFP transduced ALI cultures with respect to controls (**Fig 3C**).

170 There was a significantly higher expression of GFP in the transduced groups compared to controls.
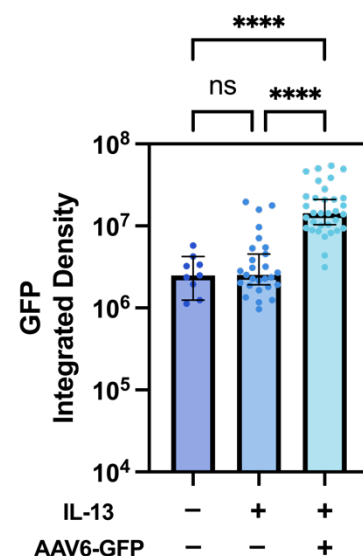

171
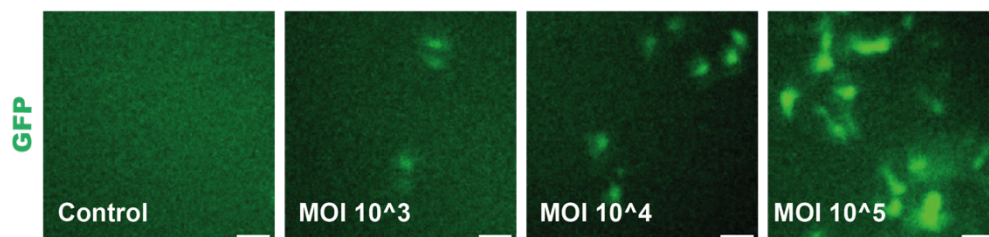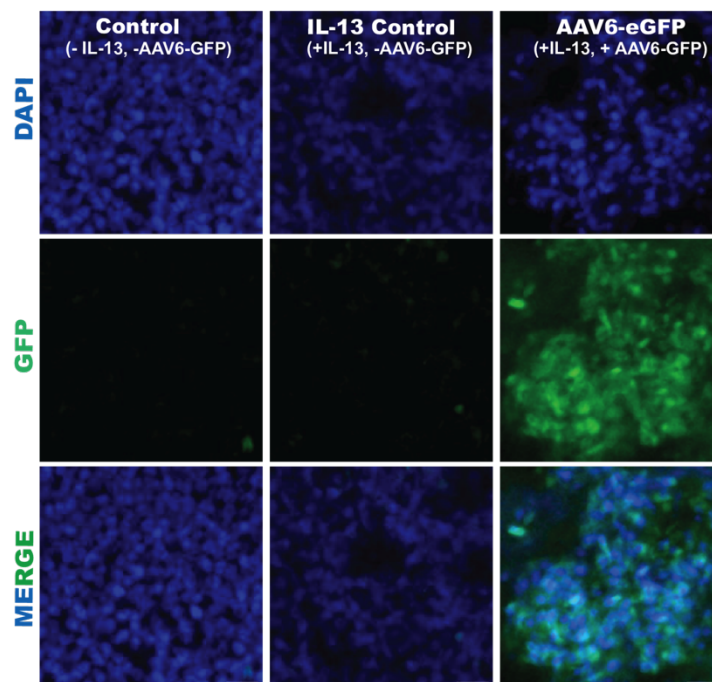
172 **Figure 3: AAV6 transduction in healthy and IL-13 treated ALI cultures *in vitro*. (A)** Representative
173 images showing AAV6-eGFP transduction in undifferentiated BCi-NS1.1 cultures at MOI of 10^3, 10^4,
174 and 10^5. Scale bar = 50 μm. **(B)** Representative images showing AAV6-eGFP transduction in IL-13

175 treated ALI cultures with respect to untransduced untreated and untransduced IL-13 treated controls. Scale
176 bar = 20 μm. **(C)** Bar graphs showing GFP integrated density in IL-13 treated AAV6-eGFP transduced ALI
177 cultures with respect to untransduced untreated and IL-13 treated controls (n=9). ****p < 0.0001 by
178 Kruskal-Wallis test with Dunn's correction. Each dot represents different images.
179

180 *AAV6 mediated delivery of MUC5AC-siRNA in IL-13 stimulated human airway epithelial cells*

181 AAVs can be effectively packaged with siRNA, which are short 21-nucleotide dsRNA molecules,

182 for gene therapy to target disease-causing genes[37]. To test the efficacy of AAV6 mediated silencing

183 of MUC5AC expression, we transduced ALI cultures with 2 doses of AAV6 carrying MUC5AC

184 siRNA (AAV6-5AC siRNA) on day 15 and day 18 of differentiation respectively, at an MOI of

185 2500 and allowed 72h for transduction for each dose. On day 21, these cultures were challenged

186 with IL-13 for 7 days. On day 28, the cultures were assessed for MUC5AC RNA and protein

187 expression (**Fig 4A**). We performed qPCR to measure MUC5AC mRNA levels and found that

188 groups treated with AAV6-5AC siRNA had comparable MUC5AC mRNA levels to untreated

189 control whereas the IL-13 treated control was ~1.5 times higher than the treated group and ~2

190 times higher than untreated control (**Fig 4B**). To measure MUC5AC and MUC5B protein

191 expression, we performed immunofluorescence staining in untreated, IL-13 treated control, and

192 AAV6-5AC siRNA treated groups and quantified the integrated density of MUC5AC and MUC5B

193 expression. There was increased MUC5AC expression in IL-13 treated controls compared to

194 untreated control and AAV6-5AC siRNA treated groups (**Fig 4C & 4D**). There was also increased

195 mucin content as reflected by the O-linked glycosylation quantification in IL-13 treated groups

196 with lower and comparable mucin content in untreated control and AAV6-5AC siRNA treated

197 group (**Fig S2**). MUC5B expression was comparable across all groups with no significant
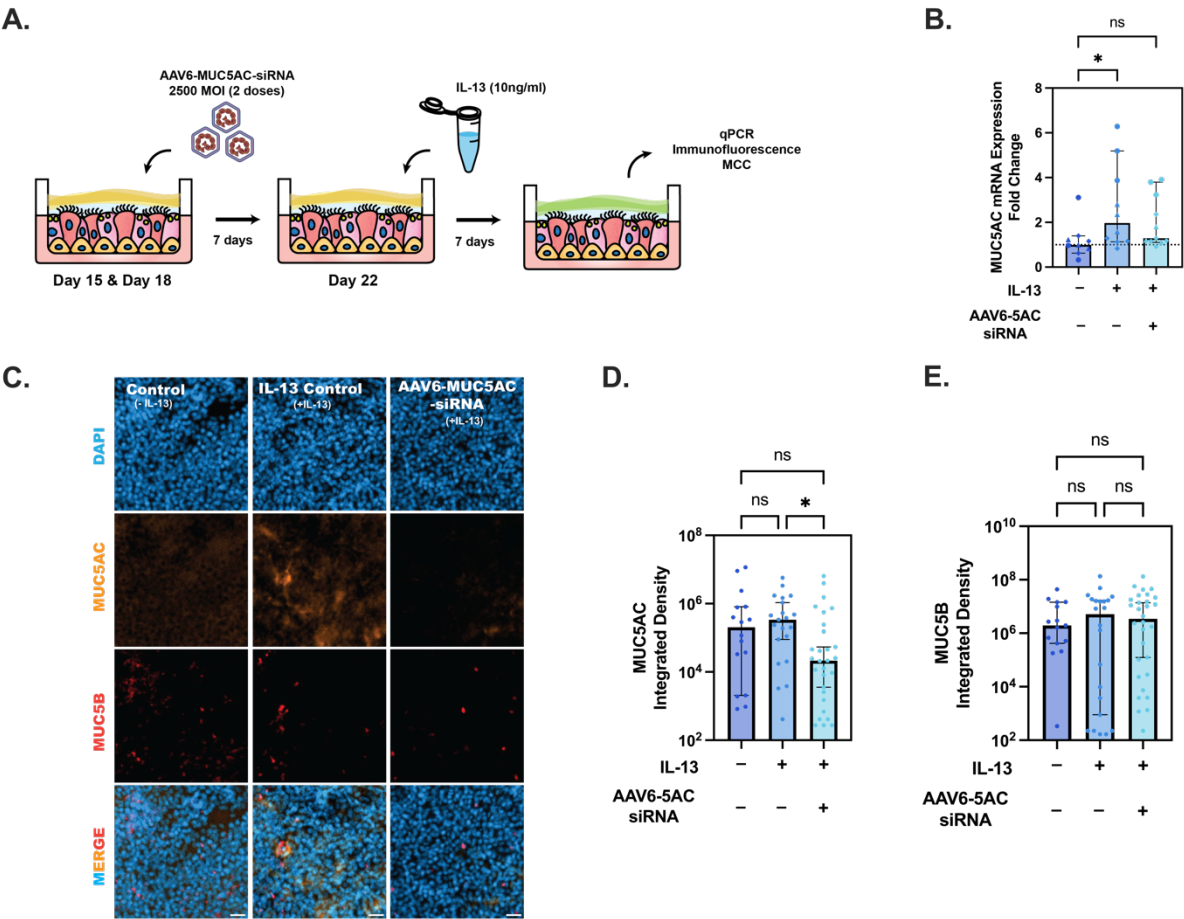
198 difference (**Fig 4C & 4E**).

199

Figure 4: AAV6 delivers MUC5AC siRNA into IL-13 treated ALI cultures. (A) Schematic illustration demonstrating 2 dose pre-treatments with 2500 MOI of AAV6 expressing MUC5AC siRNA (AAV6-5AC siRNA) in ALI cultures before challenging with IL-13. **(B)** Scatter plot showing MUC5AC mRNA fold change in IL-13 treated control and AAV6-5AC siRNA treated groups with respect to untreated control. Shapes represent different experimental trials. *$p < 0.05$ by Kruskal-Wallis test with Dunn's correction. **(C)** Representative images showing MUC5B and MUC5AC protein expression in untreated control, IL-13 treated control and AAV6-5AC siRNA treated groups. Scale bar = 25 μm. **(D-E)** Bar graphs showing MUC5AC and MUC5B integrated density respectively, measured from immunofluorescence images (n≥15, across 9-15 cultures) in untreated controls, IL-13 treated controls, and AAV6-5AC siRNA treated groups. *$p < 0.05$ by Kruskal-Wallis test with Dunn's correction.

210

Impact of AAV6 mediated MUC5AC siRNA treatment on mucociliary transport in IL-13 stimulated

human airway epithelial cell cultures

To evaluate MUC5AC as a suitable target to improve airway clearance in asthma, we measured

mucociliary transport rates following treatment with AAV6 expressing MUC5AC siRNA in IL-

13 stimulated HAE cultures. Seven days after IL-13 challenge and/or AAV6-5AC siRNA

216   treatment (**Fig 4A)**, mucociliary transport rate was measured by adding 2 μm red fluorescent beads

217   to the apical surface of transwells and the movement of the beads were tracked in real time using

218   live cell video microscopy (**Fig 5A**). We found that beads in IL-13 treated controls traversed less

219   distance compared to beads on untreated controls and AAV6-5AC siRNA treated groups, which

220   were comparable, as seen in representative trajectories (**Fig 5B**). We observed that the median

221   transport rates of the beads in each video were comparable between untreated controls and AAV6-

222   5AC siRNA treated groups and significantly reduced in IL-13 treated controls (**Fig 5C**). We next

223   wanted to determine how many beads in each video were mobile. We defined beads to be mobile

224   if they traversed a distance greater than or equal to their radii (1 μm) in 10 seconds equivalent to

225   a velocity of 0.1 μm/s. Based on this, beads with speeds less than 0.1 μm/s were considered

226   immobile or stuck (gray shaded region in **Fig 5D**). The percentage of mobile particle tracers in

227   each video was then calculated using a 0.1 μm/s velocity cutoff. We found the untreated controls

228   and AAV6-5AC siRNA treated groups had comparable mobile beads ~65% while IL-13 treated

229   controls had significantly fewer mobile beads, less than 50% were mobile (**Fig 5E**). To confirm

230   that these changes in transport rates were due to change in secreted mucin composition and not

231   ciliated epithelium function, we measured the ciliary beat frequency which was comparable in all
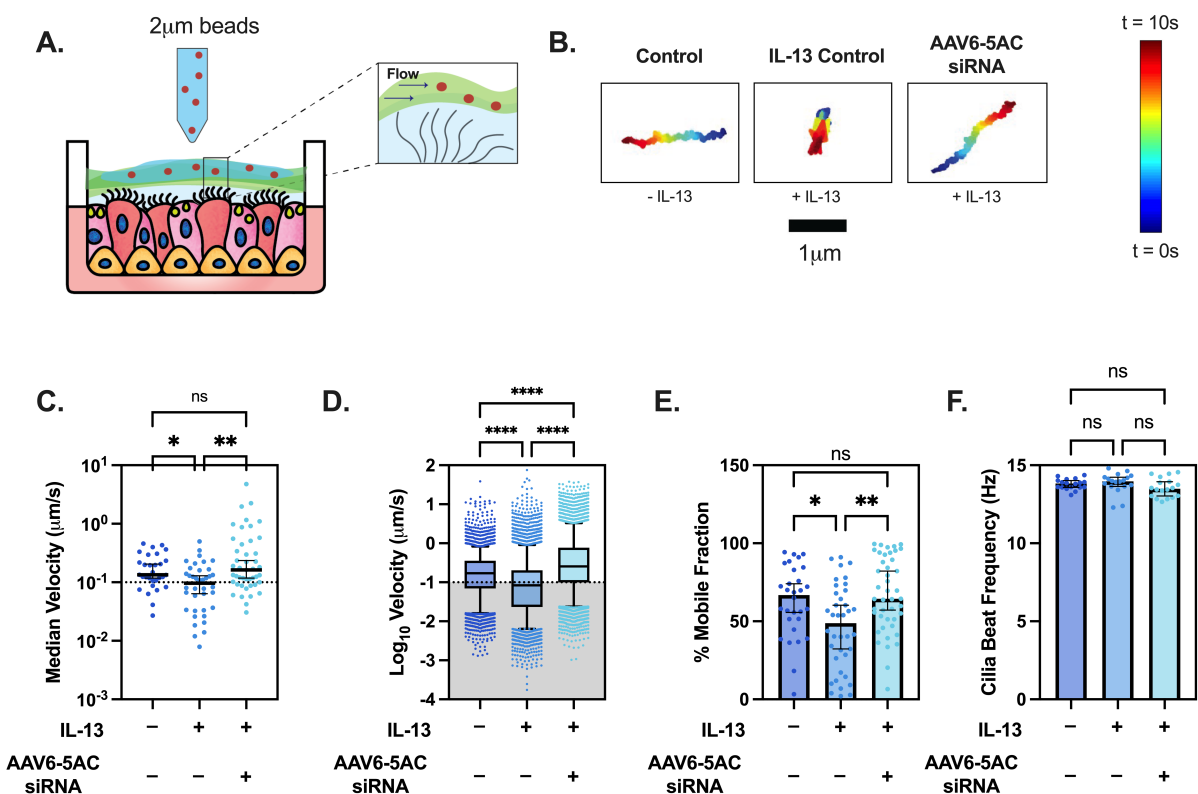
232   groups (**Fig 5F**).

Figure 5: Mucociliary transport is maintained in MUC5AC siRNA treated HAE cultures challenged with IL-13. (A) Schematic showing the design of MCT measurement. Briefly, 2 μm beads are applied onto mucus on ALI cultures. The coordinated beating of cilia causes the mucus with beads to flow, which is imaged. **(B)** Representative trajectories of single beads in untreated control, IL-13 treated control, and AAV6-5AC siRNA treated group. Dark blue represents trajectories at 0 s and dark red represents trajectories at 10 s. **(C)** Scatter plot represents median velocities (μm/s) of beads in each video for untreated control, IL-13 treated control, and AAV6-5AC siRNA groups (n = 30). **$p < 0.01$ by Kruskal-Wallis test with Dunn's correction. **(D)** Box and Whisker plot representing velocities (μm/s) of all beads in untreated control, IL-13 treated control and AAV6-5AC siRNA groups. Shaded region indicates particles with velocities < 0.1 μm/s. ****$p < 0.0001$ by Kruskal-Wallis test with Dunn's correction. **(E)** Scatter plot showing immobile fraction (no. of beads with velocity < 0.1 μm/s/ total beads) in each video for untreated control, IL-13 treated control and AAV6-5AC siRNA groups. ***$p < 0.001$ by Kruskal-Wallis test with Dunn's correction. **(F)** Bar graph showing ciliary beat frequency (Hz) in untreated control, IL-13 treated control, and AAV6-5AC siRNA groups.

Discussion

In these studies, we targeted the mucin glycoprotein MUC5AC using AAV vectors to explore its potential as an inhaled gene therapy for asthma. We first assessed the capabilities of AAV6 to successfully deliver cargo into mouse lungs and airways via intranasal administration and

254   determine if relevant epithelial subsets were transduced (e.g. mucus-secreting cells). Previous

255   studies have shown successful AAV6 transduction of airway epithelial cells[27–29], but transduction

256   in epithelial subsets have not been analyzed. We saw that AAV6 successfully transduced mucus

257   secreting airway epithelial cells in the trachea. Overall, transduction in the lungs was minimal,

258   which is to be expected for the intranasal route of administration. We anticipate higher transduction

259   in the deeper lung via intratracheal modes of administration[31] which will be tested in subsequent

260   *in vivo* efficacy studies. Detection of AAV6 transduction in goblet cells in the trachea is promising

261   and provides further rationale for using AAV6 to deliver siRNA targeting MUC5AC in asthma.

262

263   A significant biological barrier to inhaled gene delivery vectors is the pathological mucus produced

264   in diseases like asthma. We found in prior work that AAV6 can diffuse through pathological mucus

265   from individuals with CF and transduce airway epithelial cells *in vivo*[29]. Similarly, we saw that

266   AAV6 was equally diffusive in pathological *in vitro* asthma-like (i.e.., IL-13 stimulated) mucus,

267   normal mucus, and MUC5B KO (i.e., MUC5AC-rich) mucus collected from ALI cultures. AAV6

268   diffusion was lower than muco-inert nanoparticles which may possibly be due to interactions of

269   AAV6 capsid proteins with heparan sulfate terminated glycans present in airway mucus[38,39].

270   However, overall, AAV6 retained the capacity to transduce the underlying epithelium in IL-13

271   stimulated, MUC5AC-secreting HAE cultures.

272

273   Pathological viscous asthma mucus is the consequence of increased goblet cell number and

274   therefore increased MUC5AC expression[21,40]. Consistent with prior studies, we observed increased

275   mRNA and protein expression of MUC5AC in IL-13 treated cultures. Pre-treatment with AAV6

276   expressing MUC5AC siRNA was able to protect cultures when challenged with IL-13, with

277   MUC5AC expression comparable to untreated controls. This was also reflected in the

278   quantification of total O-linked glycosylation in mucus collected from each group. In terms of

279   MUC5B expression, prior literature is inconsistent, with some studies reporting increased MUC5B

280   expression in asthma[41], and others reporting no change[42]. In the current work, we observed no

281   significant differences in MUC5B protein expression between the groups and as such, MUC5AC

282   siRNA treatment did not appear to cause any compensatory expression of MUC5B.

283

284   Impaired mucociliary clearance in asthma contributes to obstruction in the airway and creates a

285   niche for exacerbation-initiating infections[19,43]. As noted, asphyxiation from complete blocking of

286   the airway by intraluminal mucus plugs is the primary cause of death in asthma[44–46]. To determine

287   the potential of the approach to restore normal MCC in asthma, we also evaluated if MUC5AC

288   siRNA delivery with AAV6 would lead to improved MCC in IL-13 stimulated HAE cultures. In

289   IL-13 treated HAE cultures pre-treated with AAV6-5AC siRNA, MCC remained effective despite

290   being challenged with IL-13 with comparable transport velocities and mobile beads to untreated

291   control. These findings suggests a prophylactic strategy to suppress MUC5AC hypersecretion

292   could be useful in preventing mucostasis and generation of airway mucus plugs in asthma.

293

294   The present study demonstrated that AAV6 is successfully able to penetrate an asthma-like mucus

295   barrier and transduce IL-13 stimulated HAE cells differentiated at ALI *in vitro*. We also showed

296   using an *in vitro* model of IL-13 induced asthma that AAV6 mediated siRNA delivery could

297   effectively prevent MUC5AC hypersecretion and mucociliary dysfunction. Our study also

298   provides rationale for development of mucin-targeted gene therapies for asthma and potentially

299   other chronic respiratory diseases using AAV6 given its capability to transduce secretory cells *in*

300   *vivo*. These studies provide the basis for our future plans to evaluate the effectiveness of AAV6

301   mediated MUC5AC siRNA treatment in an *in vivo* model of allergic asthma. A limitation of the

302   current work is this approach was only tested as a prophylactic treatment prior to establishment of

303   inflammation and mucostasis with IL-13 stimulation. Therefore, we also plan to assess if

304   MUC5AC siRNA delivery has the potential to reverse MUC5AC hypersecretion *in vitro* and *in*

305   *vivo.* Our results establish AAV gene therapy for MUC5AC-targeting siRNA delivery as an

306   attractive option to prevent mucus obstruction as a treatment for asthma.

307

308   **Materials and Methods**

309   *Cell Culture*

310   The BCi-NS1.1 immortalized human basal cell line was generously provided by Ronald Crystal

311   (Weill Cornell Medical College) and cultured based on previous methods[35,47]. MUC5B KO BCi-

312   NS1.1 cultures were generated as previously reported[35] and cultures were prepared from frozen

313   stocks for experiments. BCi-NS1.1 cells were cultured at 37°C, 5% CO_2 in a flask with

314   PneumaCult-Ex Plus expansion media (STEMCELL Technologies). At about 80% confluency the

315   cells were detached using 0.05% Trypsin-EDTA for 5 mins and seeded on 12 mm rat-tail collagen

316   type-I coated transwell inserts (StemCell Technologies) at 10,000 cells/cm^2 in Ex Plus medium

317   supplied on both the apical and basolateral compartments, until a confluent monolayer was

318   established. Once confluent, medium from the apical compartment was removed and PneumaCult-

319   ALI media (STEMCELL Technologies) was supplied only to the basolateral compartment to

320   transition the cultures into Air-Liquid Interface cultures. The cells were allowed to differentiate

321   into a pseudostratified mucociliary epithelium for 4 weeks with media changed every other day.

322   To establish an *in vitro* asthma model, ALI cultures were treated with recombinant human IL-13

323   (10 ng/ml, Peprotech) added in the basolateral compartment for 7 days.

324

325   *Mucus collection*

326   Mucus was collected from fully differentiated ALI cultures once or twice a week. PBS was added

327   to the apical surface of cultures for 30 mins at 37°C. After 30 mins, mucus washings were

328   concentrated by passing through 100kDa amicon filter and were stored at -80°C for long term

329   storage prior to usage.

330

331   *Particle Tracking Microrheology (PTM)*

332   Based on previously reported methods[48], carboxylate-modified polystyrene nanoparticles

333   (ThermoFisher) were surface modified with a 5-kDa polyethylene glycol-amine (PEG) coating to

334   ensure that these particles are non-adhesive to mucus. Size and zeta potential of the particles were

335   measured using NanoBrook Omni (Brookhaven Instruments). The nanoparticles had a

336   hydrodynamic diameter of 27.74 ± 10.99 nm. Twenty microliters of mucus was added to the

337   microscopy chamber made from vacuum-grease coated O-rings in which 1 µl of nanoparticles and

338   fluorescently labeled AAV6 respectively (~0.002% w/v) were added and allowed to incubate for

339   30 mins at room temperature. The diffusion of nanoparticles and AAV6 was measured using

340   fluorescence video imaging using Zeiss 800 LSM Microscope at 63x-water immersion objective.

341   Briefly, videos were taken for 10 s at 300ms exposure time (30 Hz) and analyzed using previously

342   developed MATLAB algorithm[49]. The mean squared displacement (MSD) for each particle for lag

343   time (τ) was calculated as $\langle MSD(\tau) \rangle = \langle [x(t+\tau)-x(t)]^2 + [y(t+\tau)-y(t)]^2 \rangle$.

344   *AAV6-eGFP Transduction In Vitro*

345   Undifferentiated BCi-NS1.1 cultures were seeded in 6 well plates. At 60-65% confluency, the cells

346   were infected with AAV6 encoding GFP (AAV6-CAG-eGFP, 10^{13} viral particles/ml, AAVner

347   Gene) at multiplicities of infection (MOI) of 1000, 10,000, and 100,000 viral particles per cell.

348   The cells were imaged on a Zeiss 800 LSM Microscope at 72 hours post infection and analyzed

349   for GFP expression. Differentiated BCi-NS1.1 cultures were transduced with AAV6-eGFP at MOI

350   100,000 apically in regular and IL-13 stimulated cultures, and the cells were fixed and imaged for

351   GFP expression after 72 hours.

352

353   *AAV6 MUC5AC siRNA Transduction In Vitro*

354   AAV6 packaged with MUC5AC siRNA (NM_001304359) was obtained from Applied Biological

355   Materials, Canada. Briefly, ALI cultures were pre-treated apically with 2500 MOI on with their 1st

356   dose on day 15 of differentiation and a second dose on day 18 of differentiation. These cultures

357   were challenged with IL-13 (10 ng/ml) supplemented to the media in the basolateral chamber from

358   day 21-28 and replenished with every media change. On day 28, the cells were analyzed using

359   PCR, immunofluorescent staining and particle velocimetry measurements of MCC.

360

361   *Immunofluorescence*

362   Differentiated and undifferentiated BCi-NS1.1 cells were fixed with 100% ice-cold methanol for

363   15 mins at 4°C. The cells were washed with PBS and blocked with 5% bovine serum albumin

364   (BSA) in 0.01% PBST for 1 hour at room temperature. For MUC5B (rabbit anti-human, Cell

365   Signaling Technologies, MA) and MUC5AC (mouse anti-human, ThermoFisher Scientific)

366   expression, the cultures were incubated with primary antibodies (1:1000) overnight at 4°C. The

367   next day, cultures were washed with PBS twice. The cultures were incubated with secondary

368 antibodies AlexaFlour 647 (anti-rabbit, 1:2000) and AlexaFlour 555 (anti-mouse, 1:2000) in PBS

369 for 1 hour at room temperature. The cultures were then washed with PBS twice. For cultures with

370 AAV6-eGFP transduction, cultures were fixed, incubated in 1 µg/ml DAPI in PBS for 15 mins at

371 room temperature, washed twice with PBS, and then mounted and imaged using Zeiss 800 LSM

372 Microscope. Quantification of integrated density of MUC5B and MUC5AC expression was

373 measured in FIJI image software using the automated thresholding function.

374

375 *qRT-PCR*

376 RNA was extracted from differentiated BCi-NS1.1 cultures using the RNeasy minikit (Qiagen)

377 based on manufacturer's protocol. cDNA from the RNA was prepared with SuperScript III

378 (Invitrogen) as per manufacturer's protocol. Quantitative PCR for MUC5AC was carried out using

379 PowerUP SYBR Green Master Mix (Applied Biosystems) using forward and reverse primers

380 (Integrated DNA Technologies).

381

382 *Mucociliary transport and ciliary beat frequency*

383 Prior to MCC and CBF analyses, cultures were washed, and mucus was allowed to accumulate for

384 24 hours. A 25 µl suspension of 2 µm red-fluorescent polystyrene microspheres (Invitrogen,

385 1:2000 dilution in PBS) was applied apically to the cultures and allowed to equilibrate at 37°C for

386 15 mins. Videos of 5 regions were recorded using the Zeiss 800 LSM Microscope at 10x at frame

387 rate of 10 Hz for 10 seconds. The microsphere tracking analysis is based on a custom MATLAB

388 algorithm[22]. The software computes the trajectories of the fluorescent microsphere in the xy-plane

389 in each frame. The displacement is calculated based on trajectories and velocity is calculated based

390 on displacement over time elapsed. To measure ciliary beat frequency, 20 second videos at frame

391 rate of 50 Hz were recorded at 10x magnification using the Zeiss 800 LSM Microscope from 3

392 random regions using brightfield. The local pixel intensity maxima were counted using custom

393 written MATLAB algorithm, which indicates beating cilia. The beat frequency was calculated by

394 dividing the number of beats over time elapsed.

395

396 *AAV6-mCherry Transduction In Vivo*

397 Six-week-old male and female BALB/c mice were purchased from Charles River Laboratories

398 (Wilmington, MA) and maintained in disease free conditions at the animal facility. The animal

399 study protocol was approved by the Institutional Animal Care and Use Committee (IACUC) of the

400 University of Maryland College Park (protocol R-MAY-22-25). AAV6 encoding mCherry

401 (AAV6-CMV-mCherry, stock: 10^13 viral particles/ml, AAVner Gene) was intranasally

402 administered to anesthetized mice at a dose of 10^{11} viral particles/mouse. The mice were monitored

403 for 2 weeks and were sacrificed on day 14. Their lungs and trachea were isolated for imaging and

404 flow cytometry analysis as described below.

405

406 *Flow Cytometry*

407 The lungs and tracheas of mice were removed and dissected on petri plates. Single cell suspension

408 of the tissues was made by digesting tissue with Collagenase IV (1mg/ml, ThermoFisher

409 Scientific), and DNAse I (25ug/ml, Millipore Sigma) for 45 minutes at 37°C. Dispase II (2mg/ml,

410 Millipore Sigma) was also added for trachea. The tissue was then repeatedly passed through a 70

411 µm cell strainer until a single cell suspension was obtained. The cells were washed in PBS (300xg,

412 5 mins) twice. The lung cells were suspended in RBC Lysis buffer for 3 mins on ice and washed

413 with PBS. The cells were distributed into groups in FACS staining buffer and were stained for

414 different airway epithelial cell markers as shown in **Table 1** and flow cytometry was performed

415 (BD FACS Celesta).

416 **Table 1.** Antibodies used for flow cytometry

Cell Marker	Primary/Conjugated Antibody	Secondary Antibody	Manufacturer
Basal Cells (CD271)	AlexaFluor 488 conjugated		eBioscience (#53-9400-42)
Ciliated Cells (α-Tubulin)	AlexaFluor 488 conjugated	-	Biolegend (#627906)
Goblet Cells (MUC5AC)	Mouse anti-MUC5AC	Anti-mouse AlexaFluor488	ThermoFisher, Biolegend (MA5-12178, 406001)
Secretory Cells (TSPAN8)	AlexaFluor 488 conjugated	-	FisherScientific (FAB6524G100)

417

418 *Ex Vivo Cryosectioning and Staining*

419 To prepare lungs and trachea for immunofluorescence, the lungs were inflated with 10% formalin

420 which was delivered through blunt-end needle inserted via the trachea. After inflation, the lungs

421 and trachea were collected and placed in 10% formalin overnight at room temperature. The tissues

422 were transferred to cryomolds with OCT and frozen at -80°C. Using the Leica CM1950 Cryostat,

423 10 µm lung sections and 7 µm tracheal sections were made. The sections were allowed to calibrate

424 at room temperature overnight and fixed with 100% methanol and stained with DAPI as per

425 immunofluorescence protocol and imaged at 10x magnification using the Zeiss 800 LSM

426 Microscope.

427

428 *Statistical Analysis*

429 The data were statistically analyzed using GraphPad Prism Software. Comparison between 2

430 groups were performed using 2-tailed student *t* test or Mann-Whitney *U* test. For comparison

431 between groups, either one-way analysis of variance (ANOVA) followed by a Tukey post hoc

432   correction was used or Kruskal-Wallis with Dunn's correction was used for non-Gaussian

433   distributions. All graphs show median values and 5th up to 95th percentiles of data and outliers

434   are included. Differences were considered statistically significant at p value < 0.05.

435

References

437   1. Braman, S. S. The Global Burden of Asthma. *Chest* **130**, 4S-12S (2006).

438   2. Dharmage, S. C., Perret, J. L. & Custovic, A. Epidemiology of Asthma in Children and

439   Adults. *Frontiers in Pediatrics* **7**, (2019).

440   3. The Global Asthma Report 2022. *int j tuberc lung dis* **26**, 1–104 (2022).

441   4. Fahy, J. V. Type 2 inflammation in asthma--present in most, absent in many. *Nat Rev

442   Immunol* **15**, 57–65 (2015).

443   5. Spellberg, B. & Edwards, J. E. Type 1/Type 2 immunity in infectious diseases. *Clin Infect Dis*

444   **32**, 76–102 (2001).

445   6. Song, D., Cahn, D. & Duncan, G. A. Mucin Biopolymers and Their Barrier Function at

446   Airway Surfaces. *Langmuir* **36**, 12773–12783 (2020).

447   7. Patel, V. H. *et al.* Current Limitations and Recent Advances in the Management of Asthma.

448   *Disease-a-Month* **69**, 101483 (2023).

449   8. Ip, M., Lam, K., Yam, L., Kung, A. & Ng, M. Decreased bone mineral density in

450   premenopausal asthma patients receiving long-term inhaled steroids. *Chest* **105**, 1722–1727

451   (1994).

452   9. Gaga, M. & Zervas, E. Oral steroids in asthma: a double-edged sword. *Eur Respir J* **54**,

453   1902034 (2019).

454 10. Boboltz, A., Kumar, S. & Duncan, G. A. Inhaled drug delivery for the targeted treatment

455   of asthma. *Advanced Drug Delivery Reviews* **198**, 114858 (2023).

456 11. Zavorotinskaya, T., Tomkinson, A. & Murphy, J. E. Treatment of experimental asthma

457   by long-term gene therapy directed against IL-4 and IL-13. *Molecular Therapy* **7**, 155–162

458   (2003).

459 12. Behera, A. K., Kumar, M., Lockey, R. F. & Mohapatra, S. S. Adenovirus-Mediated

460   Interferon γ Gene Therapy for Allergic Asthma: Involvement of Interleukin 12 and STAT4

461   Signaling. *Human Gene Therapy* **13**, 1697–1709 (2002).

462 13. Xie, Y. *et al.* Targeted delivery of siRNA to activated T cells via transferrin-

463   polyethylenimine (Tf-PEI) as a potential therapy of asthma. *Journal of Controlled Release*

464   **229**, 120–129 (2016).

465 14. Choi, M., Gu, J., Lee, M. & Rhim, T. A new combination therapy for asthma using dual-

466   function dexamethasone-conjugated polyethylenimine and vitamin D binding protein siRNA.

467   *Gene Ther* **24**, 727–734 (2017).

468 15. Thanki, K., Blum, K. G., Thakur, A., Rose, F. & Foged, C. Formulation of RNA

469   interference-based drugs for pulmonary delivery: challenges and opportunities. *Therapeutic*

470   *Delivery* **9**, 731–749 (2018).

471 16. Tanaka, M. & Nyce, J. W. Respirable antisense oligonucleotides: a new drug class for

472   respiratory disease. *Respir Res* **2**, 5–9 (2001).

473 17. Chiang, P.-C., Chen, J.-C., Chen, L.-C. & Kuo, M.-L. Adeno-Associated Virus-Mediated

474   Interleukin-12 Gene Expression Alleviates Lung Inflammation and Type 2 T-Helper-

475   Responses in Ovalbumin-Sensitized Asthmatic Mice. *Human Gene Therapy* **33**, 1052–1061

476   (2022).

477   18.   Dunican, E. M., Watchorn, D. C. & Fahy, J. V. Autopsy and Imaging Studies of Mucus

478   in Asthma. Lessons Learned about Disease Mechanisms and the Role of Mucus in Airflow

479   Obstruction. *Ann Am Thorac Soc* **15**, S184–S191 (2018).

480   19.   Dunnill, M. S. THE PATHOLOGY OF ASTHMA, WITH SPECIAL REFERENCE TO

481   CHANGES IN THE BRONCHIAL MUCOSA. *J Clin Pathol* **13**, 27–33 (1960).

482   20.   HUBER, H. L. & KOESSLER, K. K. THE PATHOLOGY OF BRONCHIAL ASTHMA.

483   *Archives of Internal Medicine* **30**, 689–760 (1922).

484   21.   Lachowicz-Scroggins, M. E. *et al.* Abnormalities in MUC5AC and MUC5B Protein in

485   Airway Mucus in Asthma. *Am J Respir Crit Care Med* **194**, 1296–1299 (2016).

486   22.   Song, D. *et al.* Modeling Airway Dysfunction in Asthma Using Synthetic Mucus

487   Biomaterials. *ACS Biomaterials Science & Engineering* (2021)

488   doi:10.1021/acsbiomaterials.0c01728.

489   23.   Bonser, L. R., Zlock, L., Finkbeiner, W. & Erle, D. J. Epithelial tethering of MUC5AC-

490   rich mucus impairs mucociliary transport in asthma. *Journal of Clinical Investigation* **126**,

491   2367–2371 (2016).

492   24.   Siddiqui, S. *et al.* Epithelial miR-141 regulates IL-13–induced airway mucus production.

493   *JCI Insight* **6**, e139019 (2021).

494   25.   Wang, J.-H., Gessler, D. J., Zhan, W., Gallagher, T. L. & Gao, G. Adeno-associated virus

495   as a delivery vector for gene therapy of human diseases. *Sig Transduct Target Ther* **9**, 1–33

496   (2024).

497   26.   Liu, D. *et al.* Adeno-associated virus therapies: Pioneering solutions for human genetic

498   diseases. *Cytokine & Growth Factor Reviews* **80**, 109–120 (2024).

499   27.   Halbert, C. L., Allen, J. M. & Miller, A. D. Adeno-Associated Virus Type 6 (AAV6)

500   Vectors Mediate Efficient Transduction of Airway Epithelial Cells in Mouse Lungs Compared

501   to That of AAV2 Vectors. *Journal of Virology* **75**, 6615–6624 (2001).

502   28.   Li, W., Zhang, L., Wu, Z., Pickles, R. J. & Samulski, R. J. AAV-6 mediated efficient

503   transduction of mouse lower airways. *Virology* **417**, 327–333 (2011).

504   29.   Duncan, G. A. *et al.* An adeno-associated viral vector capable of penetrating the mucus

505   barrier to inhaled gene therapy. *Molecular Therapy - Methods & Clinical Development* **9**,

506   296–304 (2018).

507   30.   Limberis, M. P., Vandenberghe, L. H., Zhang, L., Pickles, R. J. & Wilson, J. M.

508   Transduction Efficiencies of Novel AAV Vectors in Mouse Airway Epithelium In Vivo and

509   Human Ciliated Airway Epithelium In Vitro. *Mol Ther* **17**, 294–301 (2009).

510   31.   Kurosaki, F. *et al.* Optimization of adeno-associated virus vector-mediated gene transfer

511   to the respiratory tract. *Gene Ther* **24**, 290–297 (2017).

512   32.   Turner, J. *et al.* Goblet cells are derived from a FOXJ1-expressing progenitor in a human

513   airway epithelium. *Am J Respir Cell Mol Biol* **44**, 276–284 (2011).

514   33.   Laoukili, J. *et al.* IL-13 alters mucociliary differentiation and ciliary beating of human

515   respiratory epithelial cells. *J Clin Invest* **108**, 1817–1824 (2001).

516   34.   Koh, K. D. *et al.* Efficient RNP-directed Human Gene Targeting Reveals SPDEF Is

517   Required for IL-13-induced Mucostasis. *Am J Respir Cell Mol Biol* **62**, 373–381 (2020).

518   35.   Song, D. *et al.* MUC5B mobilizes and MUC5AC spatially aligns mucociliary transport

519   on human airway epithelium. *Science Advances* **8**, eabq5049 (2022).

520   36.   Liu, X. *et al.* Evaluation of a rapid multi-attribute combinatorial high-throughput UV-

521   Vis/DLS/SLS analytical platform for rAAV quantification and characterization. *Molecular*

522   *Therapy Methods & Clinical Development* **32**, (2024).

523   37.   Tomar, R. S., Matta, H. & Chaudhary, P. M. Use of adeno-associated viral vector for

524   delivery of small interfering RNA. *Oncogene* **22**, 5712–5715 (2003).

525   38.   Wu, Z. *et al.* Single Amino Acid Changes Can Influence Titer, Heparin Binding, and

526   Tissue Tropism in Different Adeno-Associated Virus Serotypes. *J Virol* **80**, 11393–11397

527   (2006).

528   39.   Xie, Q., Lerch, T. F., Meyer, N. L. & Chapman, M. S. Structure-function analysis of

529   receptor-binding in adeno-associated virus serotype 6 (AAV-6). *Virology* **420**, 10–19 (2011).

530   40.   Bonser, L. R. & Erle, D. J. Airway Mucus and Asthma: The Role of MUC5AC and

531   MUC5B. *J Clin Med* **6**, 112 (2017).

532   41.   Kirkham, S., Sheehan, J. K., Knight, D., Richardson, P. S. & Thornton, D. J.

533   Heterogeneity of airways mucus: variations in the amounts and glycoforms of the major

534   oligomeric mucins MUC5AC and MUC5B. *Biochem J* **361**, 537–546 (2002).

535   42.   Welsh, K. G. *et al.* MUC5AC and a Glycosylated Variant of MUC5B Alter Mucin

536   Composition in Children With Acute Asthma. *Chest* **152**, 771–779 (2017).

537   43.   Button, B. *et al.* Periciliary Brush Promotes the Lung Health by Separating the Mucus

538   Layer from Airway Epithelia. *Science* **337**, 937–941 (2012).

539   44.   Messer, J. W., Peters, G. A. & Bennett, W. A. Causes of death and pathologic findings in

540   304 cases of bronchial asthma. *Dis Chest* **38**, 616–624 (1960).

541   45.   Kuyper, L. M. *et al.* Characterization of airway plugging in fatal asthma. *Am J Med* **115**,

542   6–11 (2003).

46. Evans, C. M., Kim, K., Tuvim, M. J. & Dickey, B. F. Mucus hypersecretion in asthma: causes and effects. *Curr Opin Pulm Med* **15**, 4–11 (2009).

47. Walters, M. S. *et al.* Generation of a human airway epithelium derived basal cell line with multipotent differentiation capacity. *Respir Res* **14**, 135 (2013).

48. Schuster, B. S., Suk, J. S., Woodworth, G. F. & Hanes, J. Nanoparticle diffusion in respiratory mucus from humans without lung disease. *Biomaterials* **34**, 3439–3446 (2013).

49. Schuster, B. S., Ensign, L. M., Allan, D. B., Suk, J. S. & Hanes, J. Particle tracking in drug and gene delivery research: state-of-the-art applications and methods. *Adv Drug Deliv Rev* **91**, 70–91 (2015).

Acknowledgments

Author contributions:

Conceptualization: GAD

Methodology: SK, YC, MC, MAS, GAD

Investigation: SK, YC, MC

Visualization: SK, GAD

Supervision: MAS, GAD

Writing—original draft: SK

Writing—review & editing: SK, YC, MC, MAS, GAD

566

567   **Competing interests:** Authors declare that they have no competing interests.

568

569   **Data and materials availability:** All data are available in the main text or the

570   supplementary materials.

571